Neurobiology of Aging 123 (2023) 23–34

Contents lists available at ScienceDirect

Neurobiology of Aging

journal homepage: www.elsevier.com/locate/neuaging.org

Heterogenous response to aging of astrocytes in murine *Substantia Nigra pars compacta* and *pars reticulata*

Heather Bondi[a,b], Fausto Chiazza[a,b], Irene Masante[b], Valeria Bortolotto[a,b], Pier Luigi Canonico[b], Mariagrazia Grilli[a,b,*]

[a] *Laboratory of Neuroplasticity, University of Piemonte Orientale, Novara, Italy*
[b] *Department of Pharmaceutical Sciences, University of Piemonte Orientale, Novara, Italy*

ARTICLE INFO

Article history:
Received 28 November 2022
Accepted 21 December 2022
Available online 29 December 2022

Keywords:
Substantia nigra
Aging
Astrocytes
Glial plasticity
Morphometry
GLT1

ABSTRACT

Currently, little is known about the impact of aging on astrocytes in *substantia nigra pars compacta* (SNpc), where dopaminergic neurons degenerate both in physiological aging and in Parkinson's disease, an age-related neurodegenerative disorder. We performed a morphometric analysis of GFAP$^+$ astrocytes in SNpc and, for comparison, in the *pars reticulata* (SNpr) of young (4–6 months), middle-aged (14–17 months) and old (20–24 months) C57BL/6J male mice. We demonstrated an age-dependent increase of structural complexity only in astrocytes localized in SNpc, and not in SNpr. Astrocytic structural remodelling was not accompanied by changes in GFAP expression, while GFAP increased in SNpr of old compared to young mice. In parallel, transcript levels of selected astrocyte-enriched genes were evaluated. With aging, decreased GLT1 expression occurred only in SNpc, while xCT transcript increased both in SNpc and SNpr, suggesting a potential loss of homeostatic control of extracellular glutamate only in the subregion where age-dependent neurodegeneration occurs. Altogether, our results support an heterogenous morphological and biomolecular response to aging of GFAP$^+$ astrocytes in SNpc and SNpr.

1. Introduction

Among glial cells, astrocytes represent a highly heterogeneous population from a molecular, morphological, and functional point of view. Astrocytes are key homeostatic cells in the central nervous system. Among their pleiotropic functions, they do provide trophic support to neurons, participate in synaptic function and plasticity including uptake and recycling of neurotransmitters, regulate blood–brain barrier integrity and modulate adult neurogenesis (Spampinato et al., 2019; Verkhratsky and Nedergaard, 2018). Beyond such homeostatic functions, in response to several endogenous and exogenous signals, including potential *noxae*, astrocytes undergo profound morphological and functional changes, a process referred to as astroglial plasticity (Czéh et al., 2006; Rodríguez-Arellano et al., 2016).

Given the broad array of functions played by astrocytes, their age-related morphofunctional changes may deeply impact brain activity (Verkhratsky et al., 2020). Interestingly, it has been reported that astrocytes change their morphological structure in response to aging in a regional and sub-regional specific manner (Bondi et al., 2021; Popov et al., 2021; Rodríguez-Arellano et al., 2016). Potentially, morpho-functional heterogeneity in astrocyte response to aging may also account for selective vulnerability or resilience to neurodegeneration in distinct brain regions (Verkerke et al., 2021; Verkhratsky et al., 2016).

The *substantia nigra* (SN), a basal ganglia structure, is highly sensitive to aging (Costa, 2014). The area can be anatomically and functionally divided into 2 subregions: (1) the *pars compacta* (SNpc), enriched in dopaminergic (DA) neurons; (2) the *pars reticulata* (SNpr), a major output nucleus of basal ganglia, enriched in GABAergic neurons which receive DA from dendrites of SNpc DA neurons (Sonne et al., 2020). Progressive DAergic neuronal loss in SNpc is an inevitable physiological change that occurs with aging (Costa, 2014). A loss of more than 60% SNpc DA neurons con-

Abbreviations: ALDOC, Aldolase C; AQP4, Aquaporin 4; DA, Dopamine; GFAP, Glial Fibrillary Acidic Protein; GLAST, Glutamate Aspartate Transporter; GLT1, Glutamate Transporter-1; mGluR2, Metabotropic Glutamate Receptor 2; mGluR3, Metabotropic Glutamate Receptor 3; PD, Parkinson's Disease; PFA, Paraformaldehyde; RT-qPCR, Reverse transcription quantitative Polymerase Chain Reaction; SIP, Sholl Intersection Profile; SN, Substantia nigra; SNpc, Substantia nigra pars compacta; SNpr, Substantia nigra pars reticulata; TBS, Tris Buffer Solution; TH, Tyrosine Hydroxylase; xCT, Glutamate/cystine antiporter subunit; Y, MA, O, Young, Middle aged, Old.

* Corresponding author at: Laboratory of Neuroplasticity, Department of Pharmaceutical Sciences, University of Piemonte Orientale, Via Bovio 6, Novara, 28100, Italy.
E-mail address: mariagrazia.grilli@uniupo.it (M. Grilli).

0197-4580/$ – see front matter © 2022 Published by Elsevier Inc.
https://doi.org/10.1016/j.neurobiolaging.2022.12.010

tributes to classical motor symptoms associated to Parkinson's Disease (PD) (Collier et al., 2017). On the contrary, in SNpr neurons are relatively spared by aging and PD-associated neurodegeneration.

Very little is known about differences in astrocytic populations within SN subregions and if they are differentially affected by aging, a major risk factor for several neurodegenerative disorders, including PD (Tanner and Goldman, 1996). Herein we explored structural modifications of astrocytes in SNpc and SNpr of murine brain during aging and correlated these changes with biomolecular alterations which may potentially contribute to functional alterations in their homeostatic functions and vulnerability to neurodegeneration of SNpc DA neurons.

2. Materials and methods

2.1. Animals

Male C57BL/6J mice of 3 ages were utilized: young adult (Y, 4–6 month-old), n = 19; middle aged (MA, 14–17 month-old), n = 14; old (O, 20–24 month-old), n = 19. Mice, kept 3–4/cage with access to water and food *ad libitum,* were housed in a light- and temperature-controlled room in high-efficiency particulate air (HEPA)-filtered Thoren units (Thoren Cageing Systems) at the University of Piemonte Orientale animal facility. Animal care and handling were performed in accordance with the Italian law on animal care (D.L. 26/2014), as well as European Directive (2010/63/UE), and approved by the Organismo Preposto al Benessere Animale (OPBA) of University of Piemonte Orientale, Novara, Italy.

2.2. Tissue preparation and Immunohistochemistry

Prior to sacrifice, animals (Y, n = 6; MA, n = 8; O, n = 6) were anesthetized and transcardialy perfused with 0.9% saline solution, followed by 4% paraformaldehyde (PFA) solution as previously described (Chiazza et al., 2021). Brains were removed and post-fixed overnight in 4% PFA, followed by dehydration in sucrose gradients of 15% and 30% and sectioned coronally with a cryostat (Leica CM 1510 S) into 40 µm thick serial sections. For each animal, 3 sections from the *substantia nigra pars compacta* and *reticulata* [anterior–posterior −2.92 mm, −3.28 mm and −3.64 mm from bregma, according to mouse brain atlas (Paxinos and Franklin, 2004)] were selected. Staining was performed onto free floating sections, according to a previously published protocol (Dellarole and Grilli, 2008). Briefly, endogenous peroxidase activity was blocked with 0.3% H_2O_2 in 0.1 M TBS for 10 minute. Sections were subsequently treated at 4°C for 1 hour in a blocking solution containing 10% horse serum (HS), 0.3% Triton X-100 in 0.1 M TBS pH 7.4, and then incubated overnight at 4°C with goat polyclonal anti-GFAP antibody (cod. SC-6170, 1:100; Santa Cruz Biotechnology) or anti-tyrosine hydroxylase (TH) antibody (cod. 22941, 1:4000, Immunostar) in 2% HS, 0.1% Triton X-100 in 0.1 M TBS. The following day, sections were incubated with biotinylated horse anti-goat secondary antibody (cod. BA-9500, 1:200, Vector Laboratories) or biotinylated horse anti-mouse secondary antibody (cod. BA-2000, 1:1000, Vector Laboratories) in 2% HS in 0.1 M TBS for 1.5 hour at 4°C. Labelled cells were visualized using the ABC system (Vectastain Elite, Vector Laboratories) and with 3,3′-diaminobenzidine as chromogen (cod. D3939, Sigma-Aldrich). Nuclei were counterstained with hematoxylin (cod. H3404, Vector Laboratories).

2.3. Image acquisition and morphometric analysis

Image acquisition and morphometric analysis were performed by an operator blinded to animal group identity. Confocal 3D images were acquired using the z-stack function of a LSM700 laser-scanning confocal microscope (Carl Zeiss). Images were collected at 0.4 µm interval with a 20× objective (1024 × 1024 pixel, 8-bit depth, pixel size 0.313 µm). In each animal, 12 astrocytes per region with apparently fully intact GFAP-immunostained primary processes were selected for morphological analysis. 3D reconstructions of astrocytes were performed using FIJI software (version 1.52) with the Simple Neurite Tracer plugin (Longair et al., 2011). Sholl analysis was performed with Sholl analysis plugin consisting in counting the number of intersections between cell processes and concentric spheres emanating from the center of cell soma at fixed distances (5 µm), as previously described (Bondi et al., 2021; Ferreira et al., 2014). Sholl Intersection Profile (SIP) allows an intuitive comparison of astrocytic morphology. Moreover, 3D reconstructions were exported as SWC files and analyzed with L-measure tool to evaluate additional morphometric features (Scorcioni et al., 2008).

2.4. SNpc-SNpr dissection and mRNA/protein preparation

Mice (Y, n = 13; MA, n = 6; O, n = 13) were euthanized by cervical dislocation. Brains were rapidly removed and using a mouse brain matrix SN were isolated in each animal. In a subgroup of mice (Y, n = 6; O, n = 5), SNpc and SNpr were separated and independently collected. Once isolated, SN (total, SNpc and SNpr) were snap frozen and stocked at -80°C until use. Proteins from total SN were isolated by homogenization in RIPA buffer [Tris 50 mM, NaCl 100 mM, EGTA 5 mM, Nonidet NP-40 1%, Dithiothreitol 5 mM, Protease inhibitor cocktail (P8340, Sigma Aldrich) 10 µl/ml, PMSF 1 mM, NaF 25 mM, $NaVO_4$ 1 mM] in ice; homogenates were then incubated at 4°C for 2 hours under constant agitation. Samples were then centrifuged at 20,000 × g for 30 minute at 4°C and supernatants were collected. Proteins and mRNA from SNpc and SNpr were isolated by using AllPrep DNA/RNA/Protein Mini Kit (Qiagen, 80004) following manufacturer's instructions.

2.5. RT-qPCR

Messenger RNA concentration and purity were measured using a Nanodrop (Implen) and reverse transcribed by ImProm-II Reverse Trascription System (Promega) according to manufacturer's instructions. Real time qPCR was performed through the iTaq Universal SYBR Green Supermix (Biorad) according to manufacturer's instructions. PCR reaction was carried out with CFX Connect Real-Time PCR Detection System (Bio-Rad). Relative gene expression was obtained after normalization to housekeeping genes (S18) using the standard formula $2^{-\Delta CT}$ as previously described (Rocchio et al., 2019). Primer sequences are detailed in Table S1 (Supplementary material).

2.6. Western blot analysis

Ten micrograms of proteins for each sample were separated onto 8% acrylamide gel and then transferred to nitrocellulose membrane. After blocking (2-hour in 5% not fat dry milk in TBS 1X), membranes were incubated with mouse anti-GFAP (cod. MAB3402, 1:1000, Millipore) or mouse anti-TH (cod. 22941, 1:1000, Immunostar) overnight at 4°C and then incubated with HRP-conjugated anti-mouse secondary antibody (cod. haf018, R&D systems, 1:10000) for 1 hour at room temperature. Proteins were detected with an ECL detection system (SuperSignal West Pico PLUS Chemiluminescent Substrate, Thermo Scientific) and quantified by densitometry (ImageLab software, Biorad). Results were normalized to β-actin.

2.7. Statistical analysis

All statistical analysis and data visualizations for morphometric results were performed in RStudio version 1.2.5 (RStudio Team, 2015) using R version 3.5.1 (R Core Team, 2016) and the packages ggplot2 (Wickham, 2016), tidyverse (Wickham et al., 2019), lme4 (Bates et al., 2015) and multcomp (Hothorn et al., 2008). For statistical analysis of morphological parameters, a linear mixed effects model was used to model the data of each parameter, with age as fixed effects and animal as a random effect (with lmer function). Using this approach, it is possible to overcome the dependency of the repeated observations within each animal (Bondi et al., 2021). The presence of significant differences was tested using one-way ANOVA. SIPs were analyzed by mixed-effects nested ANOVA approach, with individual animal as random effect and radius nested within astrocytes nested within age. Statistical analysis of morphological differences between brain areas within each age-group was performed using a mixed-effect models with post hoc Tukey correction (using multcomp package). For RT-qPCR and western blot, statistical analysis and data visualizations were performed in GraphPad Prism 8. According to the number of groups, results were analyzed with Student's t-test or one-way ANOVA with Tukey's post-hoc test. For all analyses, significance was defined as $p < 0.05$. Data are presented as mean ± SEM.

3. Results

3.1. Aging affects TH and GFAP expression in murine Substantia nigra

C57Bl/6J male mice of 3 different ages were used: young (4–6 month-old, Y), middle-aged (14–17 month-old, MA) and old (20–24 month-old, O). As it can be appreciated by the immune labeling for tyrosine hydroxylase (TH), the rate-limiting dopamine synthetic enzyme, an age-dependent reduction of TH^+ cells occurred with aging in the SNpc where DAergic neurons are located (Fig. 1A). In parallel studies, western blot analysis in total SN homogenates demonstrated an age-dependent reduction of TH protein levels which reached statistical significance in old compared to young mice (Fig. 1A; Y vs. O: *p*.value = 0.03). In the same experimental groups Glial Fibrillary Acidic Protein (GFAP), a classical astrocytic protein marker, was used to label astrocytes in both subregions of the SN by immunohistochemistry (Fig. 1B). $GFAP^+$ astrocytes are more abundant in SNpr than in SNpc, and no overt change in cell density appeared to occur as a function of age. When GFAP expression levels were evaluated in total SN homogenates of different age groups, western blot analysis demonstrated a statistically significant increase in MA and O groups compared to young mice group (Fig. 1b; Y vs. MA: p value = 0.01; Y vs. O: p value = 0.006; MA vs. O: p value = 0.98).

3.2. Aging affects $GFAP^+$ astrocytic morphological complexity in SNpc, but not in SNpr

To dissect potential subregion-specific astroglial alterations in SNpc we performed a morphometric analysis on a 3-dimensional (3D) reconstruction of GFAP immune labeled astrocytes (Fig. 2A and B). As shown by SIP analysis, in the SNpc (Fig. 2C) we observed a significant increase in the number of intersections at 10–35 µm from the soma in MA as compared to Y mice. Moreover, there was a remarkable increase in the number of intersections at 5–45 µm radii in O mice as compared to both Y and MA mice (Fig. 2C). The age dependent increase in the complexity of $GFAP^+$ cells in SNpc was also confirmed by quantification of the total number, the average and the maximum number of intersections and the critical radius (the radius where maximum count of intersections occurred) (Fig. 2D, Table 1). To further confirm the increase in SNpc astrocyte complexity with aging, we also performed a quantitative analysis of a large panel of additional morphological features. The number of terminal points of astrocytes increased in an age-dependent manner (Fig. 2E, Table 1). Astrocytes from old group were characterized by a higher number of branches, primary branches, and ramification points compared with young mice group (Fig. 2E, Table 1). We also compared the length of astrocyte arborizations across ages. The total arborization length significantly increased with aging (Fig. 2E, Table 1). Similarly, the maximum process length increased with aging (Fig. 2E, Table 1). Conversely, aging did not impact on the average length of arborization branches (Fig. 2E, Table 1). To evaluate whether increased morphological complexity was paralleled by increased territory occupied by each astroglia cell, we used the 3D convex hull analysis, which measures the volume enclosed by a polygon that connects terminal points of the cellular processes. Only astrocytes belonging to the O mouse group showed a significant expansion in their volume compared to astrocytes from the other experimental groups (Fig. 2E, Table 1).

We then performed 3D reconstruction of $GFAP^+$ astrocytes in the SNpr (Fig. 3A and B). In this subregion, unlike what we observed in SNpc, Sholl analysis revealed changes neither in the SIP (Fig. 3C) nor in other complexity-related parameters (Fig. 3D, Table 1) across different ages. More detailed morphological analysis also confirmed that branching complexity of astrocytes and their volume were not different in the 3 experimental groups, suggesting no effect of aging on astrocytes within SNpr (Fig. 3E, Table 1).

3.3. Morphometric differences in SNpc versus SNpr astrocytes across ages

Since only astrocytes in the SNpc undergo structural changes with aging, we further examined astrocytic morphology in the 2 SN subregions at each individual age. In young mice, SNpc astrocytes displayed significantly longer processes and reached maximum complexity at higher distance from soma compared to those in the SNpr (Fig. 4A, Table 1). Nevertheless, SNpc and SNpr astrocyte did not differ in terms of number of branches and total length, as demonstrated by SIP comparison (Fig. 4A, Table 1). In MA mice, SIP differences between cells from SNpc and SNpr increased remarkably (Fig. 4B, Table 1). At this age, astrocytes in the SNpc displayed higher number of processes, resulting in a general increase in arborization length (Fig. 4B, Table 1). In old mice, the morphological differences between astrocytes in the SNpc and SNpr further increased, as demonstrated by comparison of SIP and other morphometric parameters (Fig. 4C, Table 1).

3.4. Aging affects substantia nigra astrocyte enriched transcripts and GFAP protein expression in a subregion-specific manner

The age-dependent morphological alterations in $GFAP^+$ astrocytes of the SNpc could possibly underlie changes in astroglial functions. In order to identify biochemical/molecular correlates that may link structural remodeling with functional changes, we isolated SNpc and SNpr from young (n = 6) and old (n = 5) mice for additional analysis. Since an age dependent increase in GFAP levels was observed in SN whole lysates, first we quantified GFAP protein levels in SNpc and SNpr of young and old mice. In the SNpc no change in GFAP protein expression was observed by western blot (Fig. 5A). Conversely, in the SNpr GFAP protein levels significantly increased in old compared to young mice (Fig. 5B, p value= 0.04). Similar changes occurred for GFAP transcript levels, as measured by RT-qPCR. Indeed, no change in GFAP expression occurred

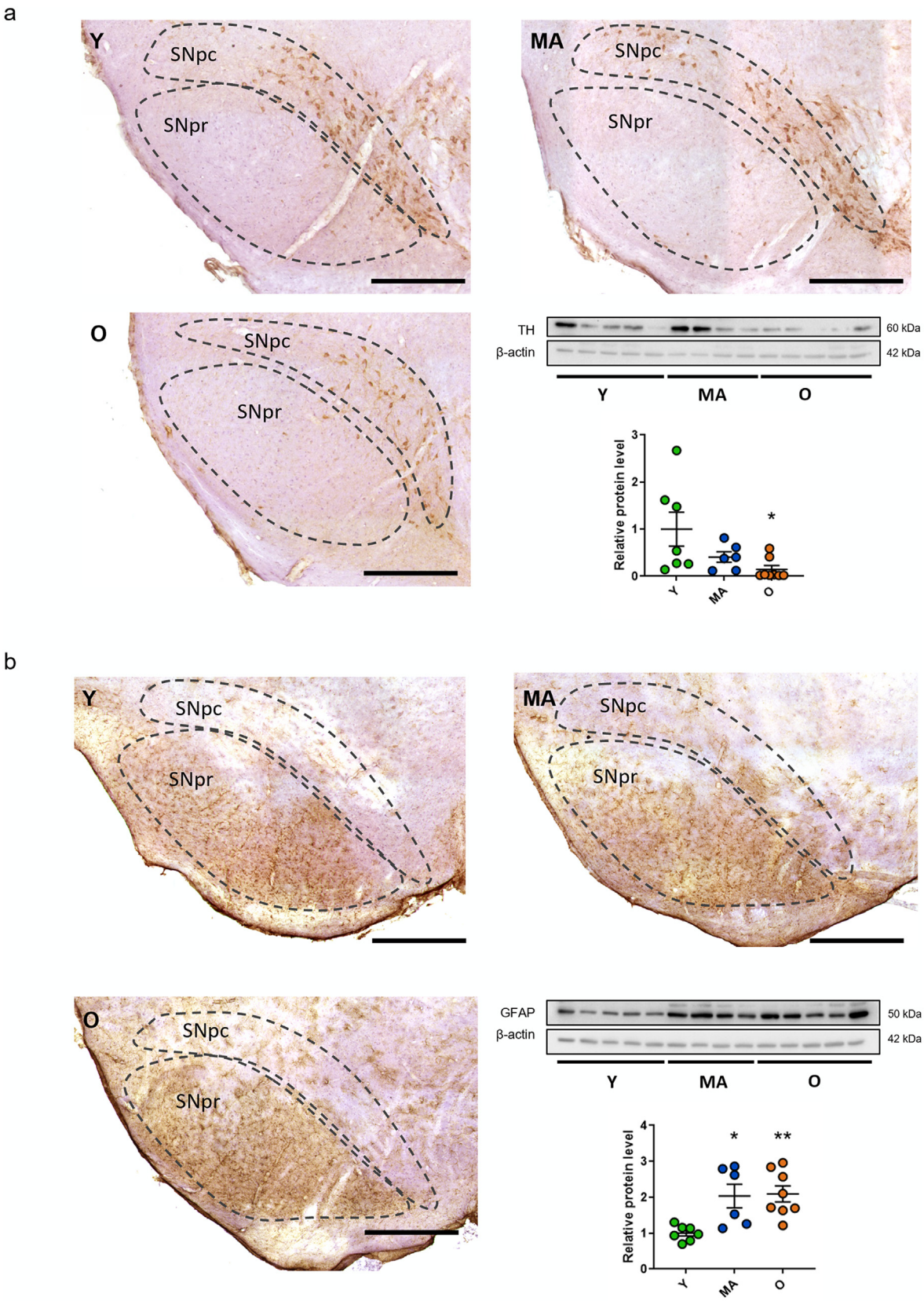

Fig. 1. (A) Representative images of tyrosine hydroxylase (TH) immunostaining of *Substantia Nigra* (SN) and Western blot analysis of TH expression levels in SN homogenates from young (Y), middle-aged (MA), and old (O) mice. (B) Representative images of glial fibrillary acidic protein (GFAP) immunostaining of SN and Western blot analysis of GFAP levels in SN homogenates from the different age groups. Data are presented as the mean ± SEM, each dot representing 1 animal. $^{*}p < 0.05$, $^{**}p < 0.05$, One-way ANOVA with Tukey's post-hoc test. Scale bars = 500 µm.

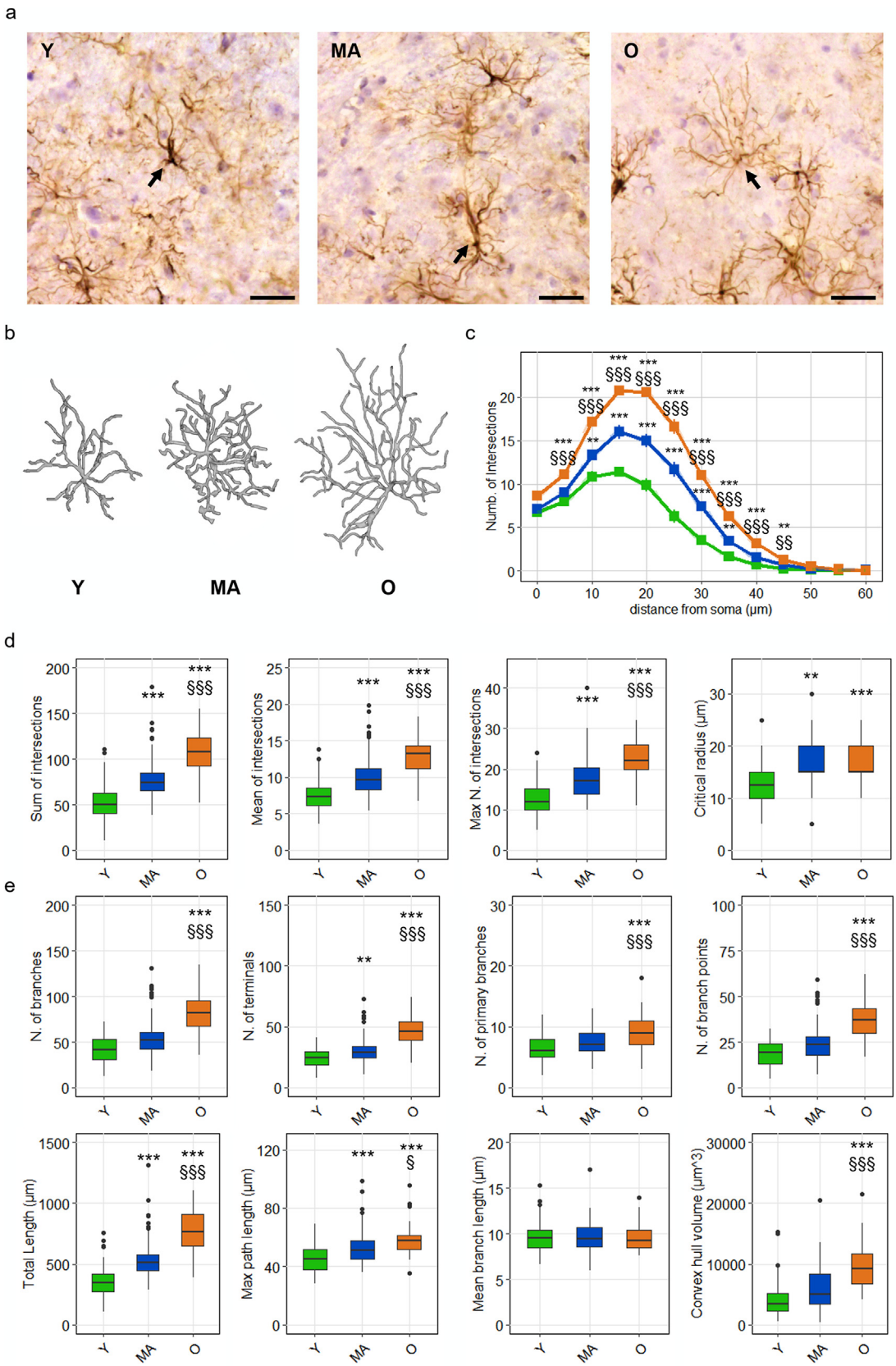

Fig. 2. In *Substantia Nigra Pars Compacta* (SNpc), morphological complexity of glial fibrillary acidic protein (GFAP)$^+$ astrocytes is increased in an age-dependent manner. (A) Representative images of GFAP$^+$ cells in the SNpc of young (Y), middle-aged (MA), and old (O) mice. Arrows indicate cells reconstructed in panel b. Scale bars= 25 µm. (B) Representative 3D reconstructions of astrocytes from young to old mice. (c) Sholl Intersection profiles (SIP) show a marked increase in branching complexity of GFAP$^+$ astrocytes with aging. Data are presented as mean ± SEM. ** $p < 0.01$, *** $p < 0.001$ versus Y; §§ $p < 0.01$, §§§ $p < 0.001$ versus MA; Nested-ANOVA followed by Tukey's HSD test on linear mixed-effect model. (D) Summary of Sholl-related parameters and (E) morphometric features describing astrocytic structural morphology. ** $p < 0.01$, *** $p < 0.001$ versus Y; §§ $p < 0.01$, §§§ $p < 0.001$ versus MA; ANOVA followed by Tukey's HSD test on linear mixed-effect model.

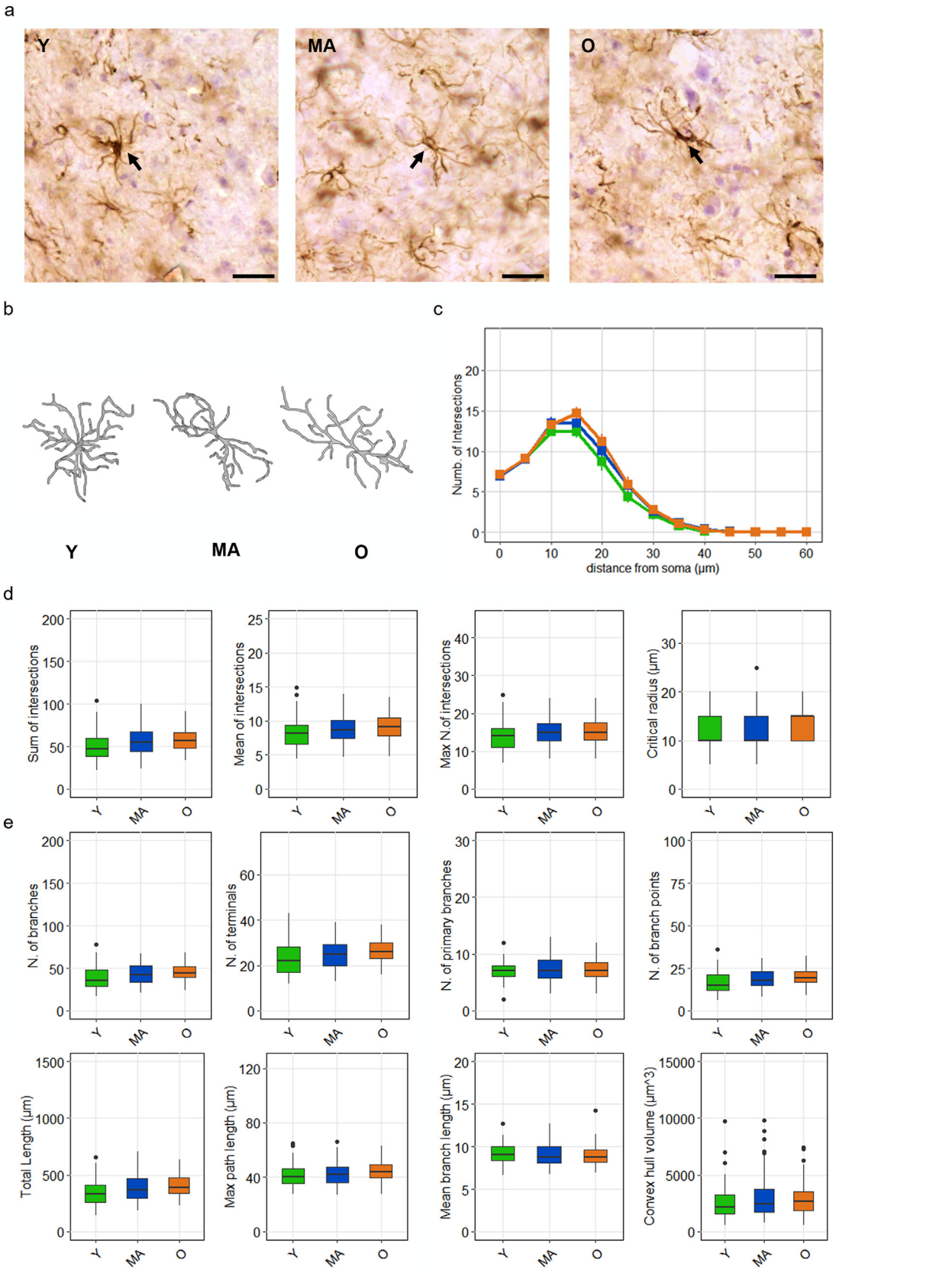

Fig. 3. In *Substantia Nigra Pars Reticulata* (SNpr), aging does not modify glial fibrillary acidic protein (GFAP)$^+$ astrocyte structure. (A) Representative images of GFAP$^+$ cells in the SNpr of young (Y), middle-aged (MA), and old (O) mice. Arrows indicate cells reconstructed in panel b. Scale bars = 25 µm. (B) Representative 3D reconstructions of astrocytes from young to old mice. (C) Sholl Intersection profiles (SIP) show no change in astrocyte complexity with aging. Data are presented as mean ± SEM. Nested-ANOVA followed by Tukey's HSD test on linear mixed-effect model. (D) Summary of Sholl-related parameters and (E) morphometric features describing astrocyte morphology. ANOVA followed by Tukey's HSD test on linear mixed-effect model.

Table 1
Summary statistics of morphometric parameters for astrocytes within *Substantia Nigra Pars compacta* (SNpc) and *Substantia Nigra Pars Reticulata* (SNpr) in young (Y), middle-aged (MA), and old (O) mice

		Y	MA	O
SNpc	Sum of Intersections	52.44 ± 19.58	78.45 ± 23.3 [b]	108.86 ± 24.45 [b,c]
	Mean of Intersections	7.52 ± 1.15	10.15 ± 2.7 [b]	12.93 ± 2.63 [b,c]
	Max Number of Intersections	12.85 ± 3.95	17.58 ± 5.5 [b]	22.68 ± 4.65 [b,c]
	Critical Radius (μm)	13.47 ± 5.15	16.09 ± 4.37 [a]	17.014 ± 4.33 [a]
	Number of Branches	41.89 ± 12.91	54.6 ± 22.39	82.85 ± 20.09 [b,c]
	Number of Tips	24.36 ± 6.9	31.11 ± 11.71 [a]	46.26 ± 10.55 [b,c]
	Number of Primary Branches	6.58 ± 2.19	7.33 ± 2.17	8.94 ± 2.83 [b,c]
	Number of Branching points	18.47 ± 6.11	24.42 ± 10.76	37.43 ± 9.72 [b,c]
	Total Branch Length (μm)	358.46 ± 130.56	541.64 ± 166.01 [b]	777.12 ± 167.81 [b,c]
	Average Branch Length (μm)	9.58 ± 1.59	9.6 ± 1.62	9.52 ± 1.32
	Max Path Length (μm)	45.47 ± 9.45	52.99 ± 10.57 [b]	57.78 ± 9.29 [b,c]
	Convex Volume (μm^3)	4205.77 ± 2842.65	5884.69 ± 3349.06	9707.43 ± 3631.4 [b]
SNpr	Sum of Intersections	50.25 ± 17.01	56.04 ± 17.48 [f]	58.39 ± 13.2 [f]
	Mean of Intersections	8.28 ± 2.3 [d]	8.81 ± 2.07 [f]	9 ± 1.94 [f]
	Max Number of Intersections	14.01 ± 3.86	15.15 ± 3.86 [f]	15.58 ± 3.29 [f]
	Critical Radius (μm)	11.88 ± 3.79 [d]	12.43 ± 4.02 [f]	13.68 ± 3.02 [f]
	Number of Branches	38.63 ± 13.31	43.26 ± 12.45 [f]	45.99 ± 10.73 [f]
	Number of Tips	22.92 ± 7.18	25.15 ± 6.74 [f]	26.65 ± 5.64 [f]
	Number of Primary Branches	7.18 ± 1.89	7.15 ± 2.41	7.3 ± 1.85 [f]
	Number of Branching points	16.57 ± 6.26 [d]	18.89 ± 5.83 [f]	20.18 ± 5.22 [f]
	Total Branch Length (μm)	41.53 ± 8.36 [e]	42.56 ± 8.80 [f]	44.72 ± 7.13 [f]
	Average Branch Length (μm)	9.15 ± 1.18	8.99 ± 1.27	8.93 ± 1.19 [e]
	Max Path Length (μm)	349.09 ± 117.23	387.47 ± 120.35 [f]	406.63 ± 92.52 [f]
	Convex Volume (μm^3)	2603.47 ± 1591.07 [d]	3026.34 ± 1953.9 [d]	2891.81 ± 1414.44 [e]

[a] $p < 0.01$,
[b] $p < 0.001$ versus Y; §§ $p < 0.01$,
[c] $p < 0.001$ versus MA; ANOVA followed by Tukey's HSD test on linear mixed-effect model.
[d] $p < 0.05$,
[e] $p < 0.01$,
[f] $p < 0.001$ versus SNpc of age-matched group; ANOVA on linear mixed-effect model.

in SNpc (Fig. 5C), whereas GFAP levels were significantly increased in SNpr of old versus young mice (Fig. 5D, p value= 0.03). Next, we extended our analysis to other astrocyte enriched transcripts. The expression of the transcript encoding the glycolytic enzyme aldolase C (AldoC) was significantly upregulated in the SNpc of old mice compared to young ones (Fig. 6A, p value= .005) and a similar trend, although not reaching significance, was confirmed in the SNpr (Fig. 6B, p value= 0.051). No statistically significant difference was observed in Aquaporin 4 (AQP4) transcript expression in both subregions of old compared to young mice (Fig 6A and B). We then focused our attention on genes involved in glutamate homeostasis, a key function of astrocytes. Interestingly, a statistically significant decrement in gene expression of the glutamate transporter GLT1 was observed in old compared to young mice only in SNpc (Fig. 6A, p. value= 0.005), but not in SNpr (Fig. 6B). Conversely, expression levels of glutamate aspartate transporter (GLAST) transcripts were similar in both SN subregions of young and old mice. We also quantified transcripts for metabotropic glutamate receptor 3 (mGluR3), an astrocyte enriched glutamate receptor, and the other group II member, metabotropic glutamate receptor 2 (mGluR2): expression levels of both transcripts were not significantly different in old versus young mice in SNpc and SNpr subregions (Fig. 6A and B). Finally, we evaluated expression levels of the glutamate/cystine antiporter subunit (xCT) transcript. xCT was significantly increased in both SNpc (Fig. 6A, p value= 0.0003) and SNpr (Fig. 6B, p value= 0.0004) of old mice, compared to young ones.

4. Discussion

Herein we describe, for the first time, a subregion-specific structural remodeling of SN astrocytes during mouse aging.

Analysis was performed in animals of 3 age ranges: 4–6, 14–17, 20–24 month old. In the 3 experimental groups we performed a morphometric analysis of astrocytes in SNpc and SNpr subregions. To this purpose, astrocyte 3D reconstructions were obtained using GFAP immune labeling. It is well established that GFAP is mainly expressed in the larger cell processes of mature astrocytes and not in fine processes such as peri-synaptic processes (Reichenbach et al., 2010). Despite such limitations, this labelling approach has been commonly used for comparative analysis of key morphometric features of astrocytes by several groups (Bondi et al., 2021; Klein et al., 2020; Olabarria et al., 2010; SheikhBahaei et al., 2018; Yeh et al., 2011). Our morphometric analysis confirmed that $GFAP^+$ astrocytes undergo a significant increase in their morphological complexity only in the SNpc, and not in the SNpr, as demonstrated by SIP comparison in mice at different ages. In *pars compacta* we also observed an increase in parameters such as number of branches, ramification and terminal points, maximum length and overall arborization length of astrocytes. Importantly, such remarkable morphological changes occurred in SNpc in parallel with age-dependent reduction of TH immunoreactivity and protein expression levels, a correlate of DAergic neuron dysfunction. Interestingly, we also demonstrated that although morphological complexity of SNpc and SNpr astrocytes is similar in 4–6 month old mice their morphological profiles diverge with increasing age. This observation strengthens the idea that in substantia nigra $GFAP^+$ astrocytes undergo structural remodeling in a strictly subregion-specific manner in response to aging.

Of note, increased morphological complexity in SNpc astrocytes with aging was not paralleled by increased GFAP expression. Although GFAP protein levels in total SN extracts were significantly augmented as a function of age and in line with previous observations even in human brain (Venkateshappa et al., 2012), the astrocytic marker increased only in SNpr, and not in SNpc, of old compared with young mice. Similar changes were also observed for GFAP transcript levels in old versus young mice. The lack

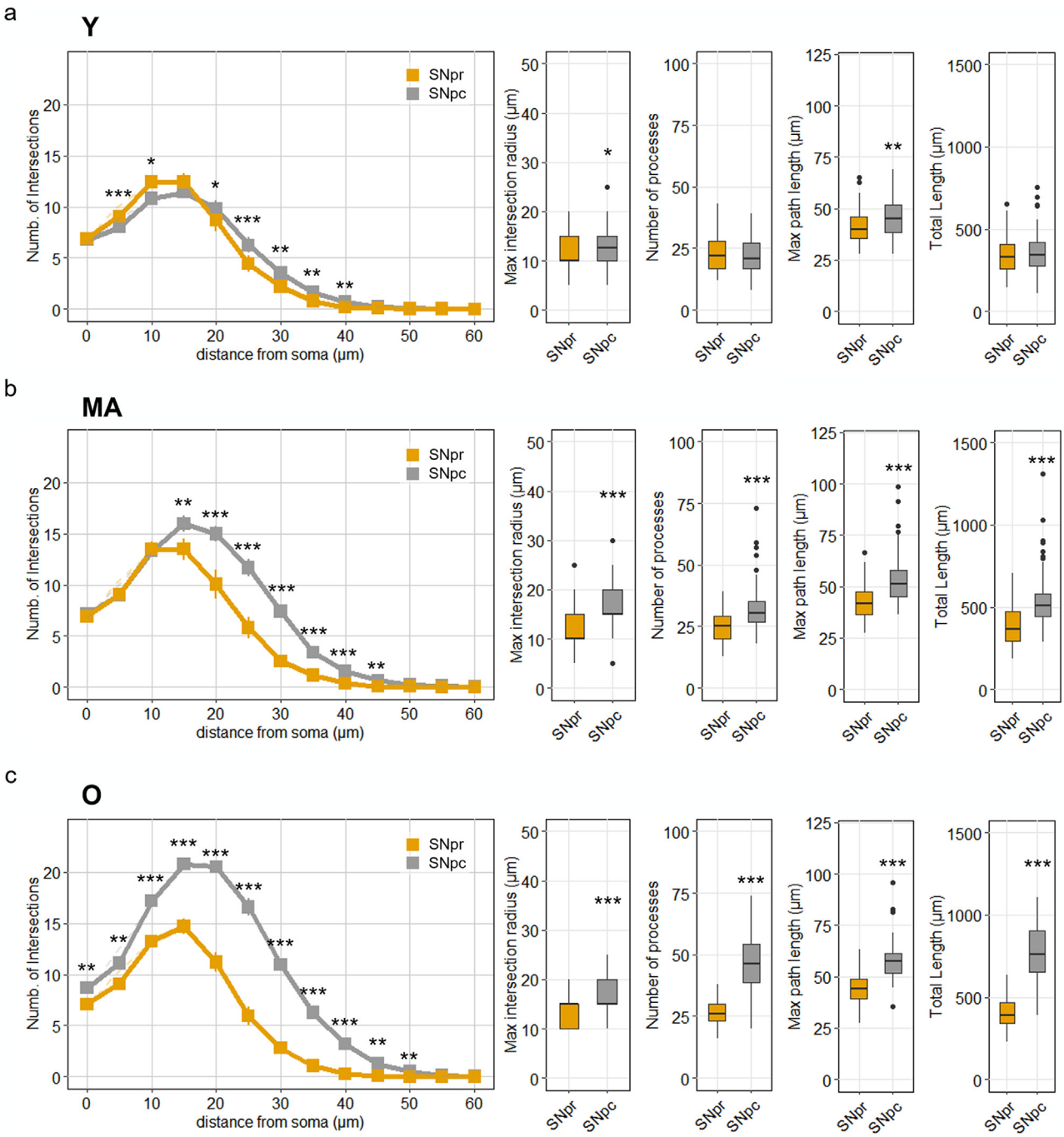

Fig. 4. Comparison across ages of astrocytic morphology in *Substantia Nigra Pars compacta* (SNpc) versus *Substantia Nigra Pars Reticulata* (SNpr). Sholl Intersection profiles (SIP) and summary of relevant parameters of astrocytes describing astrocyte morphology in (A) young, (B) middle-aged, and (C) old mice. For SIP, data are presented as mean ± SEM. * $p < 0.05$, ** $p < 0.01$, *** $p < 0.001$ versus SNpr; Nested-ANOVA on linear mixed-effect model. For box plots, * $p < 0.05$, ** $p < 0.01$, *** $p < 0.001$ versus SNpr; ANOVA on linear mixed-effect model. young = Y, middle-aged = MA, and old = O.

of correlation between GFAP$^+$ astrocyte remodeling and changes in GFAP expression levels with aging is not surprising since it was previously observed in other brain areas (Cerbai et al., 2012; Verkhratsky et al., 2020).

Recent studies have tried to understand astrocyte heterogeneous response to aging by applying state of the art omic approaches. For example, transcriptomic studies demonstrated that astrocytes from distinct brain regions of aged murine and human brain tissues have distinctive molecular signatures (Clarke et al., 2018; Soreq et al., 2017). Of note, these studies proved that in aging the most dramatic changes in gene expression profiles occur not in neurons but in glia, especially in astrocytes and oligodendrocytes (Soreq et al., 2017). Moreover, such changes mainly took place in brain areas such as human hippocampus and *substantia nigra*, incidentally 2 brain regions mostly affected by age-dependent neurodegeneration (Soreq et al., 2017). These findings provide further insights into the potential role of astrocytes, when dysfunctional, in region-specific neuronal vulnerability, a feature of age-related neurodegenerative diseases. No previous transcriptional studies are available to address molecular signatures of astrocytes

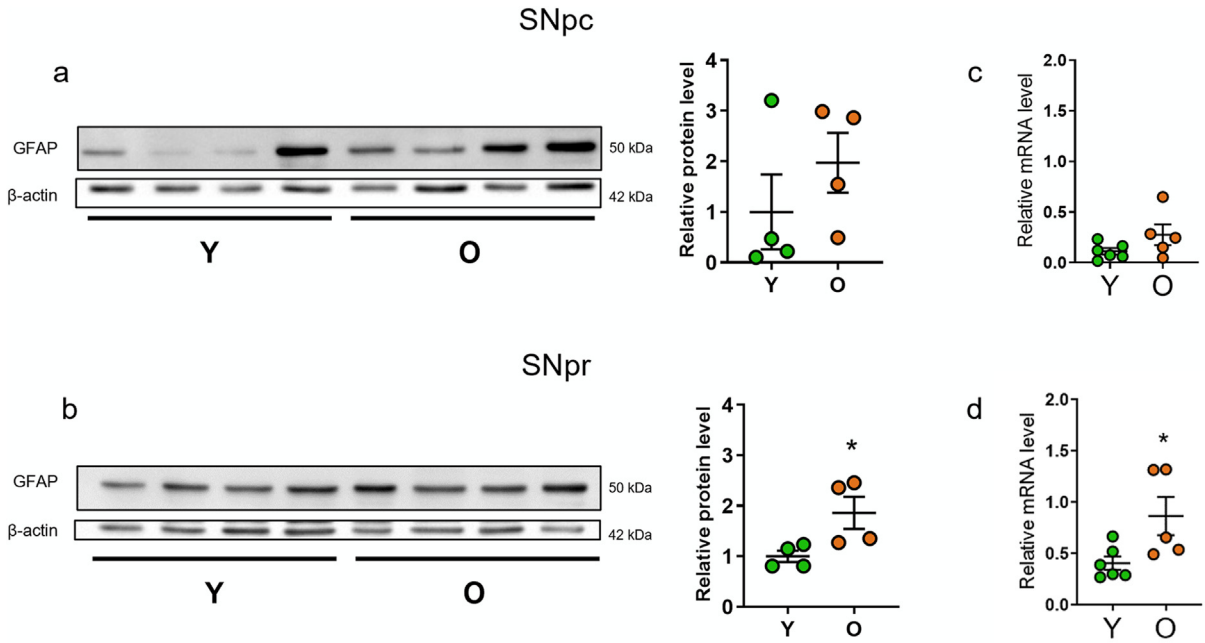

Fig. 5. Representative Western blots and relative densitometric quantification of GFAP expression levels in (A) *Substantia Nigra Pars compacta* (SNpc) and (B) *Substantia Nigra Pars Reticulata* (SNpr) of young (Y) and old mice (O). RT-qPCR analysis of GFAP transcripts in (C) SNpc and (D) SNpr. Data are presented as the mean ± SEM, each dot representing 1 animal. * $p < 0.05$; Unpaired *t*-tests. RT-qPCR, Reverse transcription quantitative Polymerase Chain Reaction.

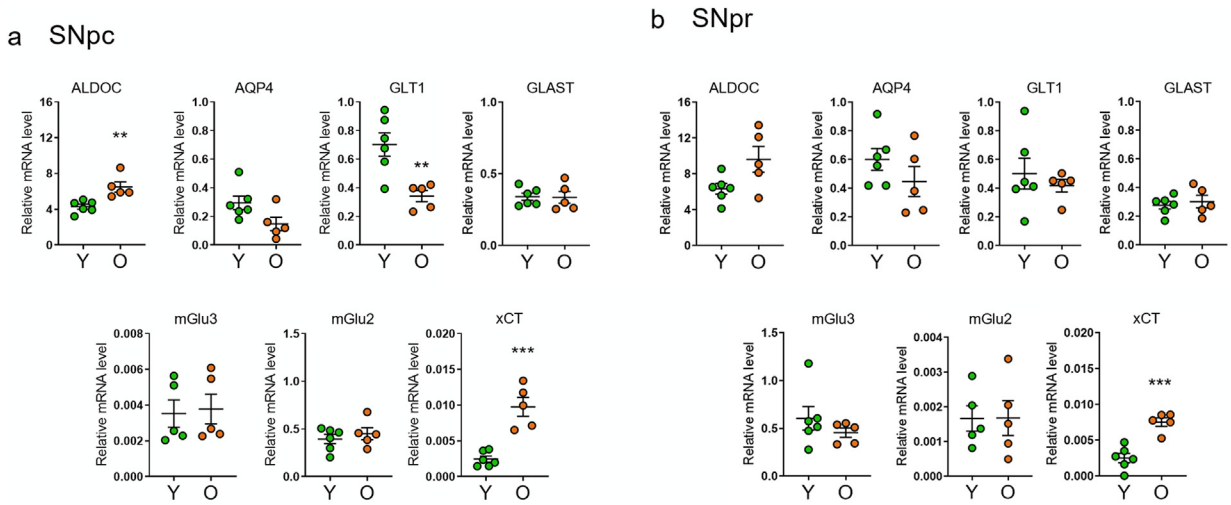

Fig. 6. RT-qPCR analysis of astroglial enriched transcripts in (A) *Substantia Nigra Pars compacta* (SNpc) and in (B) *Substantia Nigra Pars Reticulata* (SNpr) of young (Y) and old (O) mice. Data are presented as the mean ± SEM, with each dot representing 1 animal. ** $p < 0.01$, *** $p < 0.001$; Unpaired *t*-tests. Abbreviation: RT-qPCR, Reverse transcription quantitative Polymerase Chain Reaction

in SN *pars compacta* and *pars reticulata*. In our study, we attempted to correlate subregion-specific changes in astrocytic morphology with age-related biomolecular changes in the expression of selected astrocyte-enriched transcripts. It is well established that astrocytes are key actors for glutamate turnover/homeostasis in the brain. Neurons, indeed, are unable of *de novo* glutamate synthesis and they rely on astrocytes for continuous glutamine supply (Hertz and Rothman, 2017). Moreover, astrocytes express excitatory amino acid transporters 1 and 2 (EAAT1/GLAST and EAAT2/GLT1) which clear approximately 80% of glutamate released as neurotransmitter in synaptic clefts (Levy et al., 1995; Magi et al., 2019), thereby preventing the occurrence of excitotoxic events. Recent stereological studies in adult rats have attempted to gain information about the organization of astrocytes and excitatory synapses in substantia nigra (Kessler et al., 2020). These morphometric studies demonstrated a very high ratio of GLT1 expressing glial membranes to glutamatergic synapses both in SNpc and SNpr, suggesting an efficient control of extracellular glutamate concentrations in the 2 subregions. Interestingly, in our current study, we observed a decrease of GLT1 gene expression occurring only in SNpc, and not in SNpr, in old compared to young mice. In principle, subregion-specific GLT1 dysfunction could potentially lead to extracellular glutamate accumulation that might result, in turn, in increased neuronal degeneration. In our study, we also quantified cysteine-glutamate exchanger (xCT) gene expression in both SN subregions in old compared to young mice. The xCT protein is

a subunit of the x_c (-) system, an antiporter that exchanges intracellular glutamate for extracellular cysteine, thereby promoting glutathione (GSH) synthesis as well as non-vesicular glutamate release. xCT is predominantly expressed in glial cells, especially microglia and astrocytes (Ottestad-Hansen et al., 2018). Malfunctioning of the xCT system has been suggested to cause oxidative stress and excitotoxicity, both important phenomena in the pathogenesis of several neurological and neurodegenerative disorders, including PD (Lewerenz et al., 2013). Of note, mice lacking xCT were less susceptible to 6-hydroxydopamine (6-OHDA)-induced neurodegeneration in the SNpc compared to age-matched wild-type littermates (Massie et al., 2011). Reduced sensitivity to 6-OHDA might be related to marked reduction in striatal extracellular glutamate levels which was reported in mice lacking xCT (Massie et al., 2011). To our knowledge, although preliminary, our data are the first demonstration that xCT expression may be increased in SN with aging. Interestingly, we did not observe changes in expression levels of transcripts encoding other key proteins involved in the modulation of glutamate neurotransmission, such as mGluR2 and mGluR3 receptors, in both SN subregions of old mice compared to the young counterpart. We also detected a significant increase in Aldolase C (AldoC) transcripts in the SNpc of old compared to young mice, with a similar trend in the SNpr. AldoC is a brain-specific protein, expressed mainly in astrocytes (Fujita et al., 2014), which is involved in glycolysis but also in non-canonical functions, including cytoskeletal rearrangement (Merkulova et al., 2011; Volker and Knull, 1997) which is essential for structural remodeling. At the current state of knowledge, functional implications of AldoC transcript changes during aging and in SN are not understood.

Age-dependent increase in astrocyte complexity has been commonly regarded as a hallmark of astroglia reactivity (Schiweck et al., 2018). Recently the prevalent and "classical" concept of an age-dependent increase in reactive astrogliosis has been revised. At present a vast array of data support indeed the idea that astrocytic asthenia or atrophy more often contribute to aging of the brain (Popov et al., 2021; Verkhratsky et al., 2021, 2020). Altogether, it is currently envisioned that during aging astrocytic changes may also contribute to brain dysfunction through initiation and propagation of neuroinflammation (Clarke et al., 2018), oxidative stress and mitochondrial dysfunction (Acioglu et al., 2021), but mainly through reduction and/or loss in their homeostatic functions including neurotransmitter uptake and gliotransmitter release (Piacentini et al., 2017; Popov et al., 2021; Verkhratsky et al., 2021, 2020). GLT1 expression, which we found to be decreased only in SNpc and not in SNpr, has been shown to be downregulated in reactive astrocytes (Sheldon and Robinson, 2007). The increase in GFAP protein levels has been commonly related to astroglial reactivity (Eng et al., 2000) and associated to aging brain (Verkerke et al., 2021). Conversely, in our study increased morphological complexity of astrocytes in SNpc did not correlate with increased GFAP protein expression, which rather occurred in SNpr where astrocytic morphology was not affected by aging. Once again, these data support the idea that a rigid categorization of morphofunctional and molecular changes occurring in astrocytes is difficult and more complex than we can envision. Moreover, during aging structural and transcriptional changes occurring in astrocytes differ among brain regions (Boisvert et al., 2018; O'Callaghan and Miller, 1991; Rodríguez et al., 2014). For example, in striatum and hippocampus astrocytes increase their expression of GFAP and become more hypertrophic with aging. In contrast, astrocytes in the entorhinal cortex are atrophic in the aged mice (Bondi et al., 2021; Rodríguez et al., 2014). Moreover, hippocampal but not cortical astrocytes upregulate genes which are abundant in reactive astrocytes (Clarke et al., 2018). How such differences in astrocytes across different brain regions contribute to circuit function and dysfunction during aging is still largely unknown (Lawal et al., 2022). Our current data now point to sub region-specific differences in the response to aging of astrocytes in *substantia nigra* as well.

At present the full relevance of our morphometric and biomolecular data for astrocytes in SNpc is limited by their correlative nature. Despite that, we can hypothesize that age-related changes in SNpc both at the morphological and molecular levels may be associated with functional modifications of $GFAP^+$ astrocytes. Loss of homeostatic, protective functions like extracellular glutamate control could be hypothesized based on selective changes in GLT1 expression in the sub region. On the other hand, we cannot rule out the possibility that acquisition of detrimental functions may take place as a consequence of remodeling of $GFAP^+$ astrocytes only in the SNpc, where age-dependent neurodegeneration occurs. Indeed, a vast array of studies demonstrated that astrocytes not only exert a supportive role in neuronal circuitries, but they may also play an active role in age-related neurodegeneration (Acioglu et al., 2021; Colombo and Farina, 2016; Reid and Kuipers, 2021; Verkerke et al., 2021; Verkhratsky et al., 2020). The fact that these changes occur only in SNpc and not in *pars reticulata* certainly deserves further investigation, in particular to understand the impact of these changes on neuronal functions.

In conclusion, our current data support, once again, the remarkable degree of heterogeneity at any level, morphological and molecular, within astrocytic populations. Moreover they contribute to increase the current knowledge and interest on the impact of physiological aging on astrocytes in a brain region which is closely linked to age-dependent neurodegeneration (Jinno, 2011; Mosher and Schaffer, 2018).

Data availability

All data are available upon request.

Authors contribution

H.B. contributed to design research plan, performed IHC and morphometric analysis, acquired and processed images and figures, contributed to discussion, and wrote the manuscript; F.C. contributed to Western Blot and qPCR analysis, contributed to discussion and wrote the manuscript. I.M. performed acquisition of IHC images; V.B. contributed to discussion; P.L.C. provided expertise and resources and contributed to discussion; M.G. conceived, designed, and coordinated the research plan, wrote and edited the manuscript.

Submission declaration and verification

The authors declare that this paper has not been submitted elsewhere and will not be submitted elsewhere while under consideration at Neurobiology of Aging. If accepted, it will not be published elsewhere in the same form, in English or in any other language, including electronically without the written consent of the copyright-holder.

Publication of this work has been approved by all authors.

Disclosure statement

The authors report no conflicts of interest.

Acknowledgements

This work was supported by MIUR Progetti di Ricerca di Rilevante Interesse Nazionale (PRIN) Bando 2017 - grant 2017XZ7A37 to M.G.

Supplementary materials

Supplementary material associated with this article can be found, in the online version, at doi:10.1016/j.neurobiolaging.2022.12.010.

References

Acioglu, C., Li, L., Elkabes, S., 2021. Contribution of astrocytes to neuropathology of neurodegenerative diseases. Brain Res 1758. doi:10.1016/J.BRAINRES.2021.147291.

Bates, D., Mächler, M., Bolker, B.M., Walker, S.C., 2015. Fitting linear mixed-effects models using lme4. J. Stat. Softw. 67. doi:10.18637/jss.v067.i01.

Boisvert, M.M., Erikson, G.A., Shokhirev, M.N., Allen, N.J., 2018. The aging astrocyte transcriptome from multiple regions of the mouse brain. Cell Rep 22, 269–285. doi:10.1016/j.celrep.2017.12.039.

Bondi, H., Bortolotto, V., Canonico, P.L., Grilli, M., 2021. Complex and regional-specific changes in the morphological complexity of GFAP+ astrocytes in middle-aged mice. Neurobiol. Aging 100, 59–71. doi:10.1016/j.neurobiolaging.2020.12.018.

Cerbai, F., Lana, D., Nosi, D., Petkova-Kirova, P., Zecchi, S., Brothers, H.M., Wenk, G.L., Giovannini, M.G., 2012. The neuron-astrocyte-microglia triad in normal brain ageing and in a model of neuroinflammation in the rat hippocampus. PLoS One 7. doi:10.1371/journal.pone.0045250.

Chiazza, F., Bondi, H., Masante, I., Ugazio, F., Bortolotto, V., Canonico, P.L., Grilli, M., 2021. Short high fat diet triggers reversible and region specific effects in DCX^{+} hippocampal immature neurons of adolescent male mice. Sci. Rep. 11. doi:10.1038/s41598-021-01059-y.

Clarke, L.E., Liddelow, S.A., Chakraborty, C., Münch, A.E., Heiman, M., Barres, B.A., 2018. Normal aging induces A1-like astrocyte reactivity. Proc. Natl. Acad. Sci. U. S. A. 115, E1896–E1905. doi:10.1073/pnas.1800165115.

Collier, T.J., Kanaan, N.M., Kordower, J.H., 2017. Aging and Parkinson's disease: different sides of the same coin? Mov. Disord. 32, 983–990. doi:10.1002/MDS.27037.

Colombo, E., Farina, C., 2016. Astrocytes: key regulators of neuroinflammation. Trends Immunol 37, 608–620. doi:10.1016/j.it.2016.06.006.

Costa, K.M., 2014. The effects of aging on substantia nigra dopamine neurons. J. Neurosci. 34, 15133–15134. doi:10.1523/JNEUROSCI.3739-14.2014.

Czéh, B., Simon, M., Schmelting, B., Hiemke, C., Fuchs, E., 2006. Astroglial plasticity in the hippocampus is affected by chronic psychosocial stress and concomitant fluoxetine treatment. Neuropsychopharmacology 31, 1616–1626. doi:10.1038/sj.npp.1300982.

Dellarole, A., Grilli, M., 2008. Adult dorsal root ganglia sensory neurons express the early neuronal fate marker doublecortin 511, 318–328.

Eng, L.F., Ghirnikar, R.S., Lee, Y.L., 2000. Glial fibrillary acidic protein: GFAP-thirty-one years (1969-2000). Neurochem. Res. 25, 1439–1451. doi:10.1023/A:1007677003387.

Ferreira, T.A., Blackman, A.V., Oyrer, J., Jayabal, S., Chung, A.J., Watt, A.J., Sjöström, P.J., Van Meyel, D.J., 2014. Neuronal morphometry directly from bitmap images. Nat. Methods 11, 982–984. doi:10.1038/NMETH.3125.

Fujita, H., Aoki, H., Ajioka, I., Yamazaki, M., Abe, M., Oh-Nishi, A., Sakimura, K., Sugihara, I., 2014. Detailed expression pattern of Aldolase C (Aldoc) in the cerebellum, retina and other areas of the CNS studied in aldoc-venus knock-in mice. PLoS One 9, e86679. doi:10.1371/journal.pone.0086679.

Hertz, L., Rothman, D., 2017. Glutamine-glutamate cycle flux is similar in cultured astrocytes and brain and both glutamate production and oxidation are mainly catalyzed by aspartate aminotransferase. Biology (Basel) 6, 17. doi:10.3390/biology6010017.

Hothorn, T., Bretz, F., Westfall, P., 2008. Simultaneous inference in general parametric models. Biometrical J doi:10.1002/bimj.200810425.

Jinno, S., 2011. Regional and laminar differences in antigen profiles and spatial distributions of astrocytes in the mouse hippocampus, with reference to aging. Neuroscience 180, 41–52. doi:10.1016/j.neuroscience.2011.02.013.

Kessler, J., Salin, P., Kerkerian-Le Goff, L., 2020. Glutamate transporter 1-expressing glia in the rat substantia nigra—Morphometric analysis and relationships to synapses. Glia 68, 2028–2039. doi:10.1002/glia.23823.

Klein, M., Lohr, C., Droste, D., 2020. Age-dependent heterogeneity of murine olfactory bulb astrocytes. Front. Aging Neurosci. 12, 1–11. doi:10.3389/fnagi.2020.00172.

Lawal, O., Ulloa Severino, F.P., Eroglu, C., 2022. The role of astrocyte structural plasticity in regulating neural circuit function and behavior. Glia 70, 1467–1483. doi:10.1002/GLIA.24191.

Levy, L.M., Lehre, K.P., Walaas, S.I., Storm-Mathisen, J., Danbolt, N.C., 1995. Down-regulation of glial glutamate transporters after glutamatergic denervation in the rat brain. Eur. J. Neurosci. 7, 2036–2041. doi:10.1111/j.1460-9568.1995.tb00626.x.

Lewerenz, J., Hewett, S.J., Huang, Y., Lambros, M., Gout, P.W., Kalivas, P.W., Massie, A., Smolders, I., Methner, A., Pergande, M., Smith, S.B., Ganapathy, V., Maher, P., 2013. The cystine/glutamate antiporter system x c − in health and disease: from molecular mechanisms to novel therapeutic opportunities. Antioxid. Redox Signal. 18, 522–555. doi:10.1089/ars.2011.4391.

Longair, M.H., Baker, D.A., Armstrong, J.D., 2011. Simple Neurite Tracer: open source software for reconstruction, visualization and analysis of neuronal processes. Bioinformatics 27, 2453–2454. doi:10.1093/bioinformatics/btr390.

Magi, S., Piccirillo, S., Amoroso, S., Lariccia, V., 2019. Excitatory Amino Acid Transporters (EAATs): glutamate transport and beyond. Int. J. Mol. Sci. 20, 5674. doi:10.3390/ijms20225674.

Massie, A., Schallier, A., Kim, S.W., Fernando, R., Kobayashi, S., Beck, H., Bundel, D.De, Vermoesen, K., Bannai, S., Smolders, I., Conrad, M., Plesnila, N., Sato, H., Michotte, Y., 2011. Dopaminergic neurons of system x c − -deficient mice are highly protected against 6-hydroxydopamine-induced toxicity. FASEB J 25, 1359–1369. doi:10.1096/fj.10-177212.

Merkulova, M., Hurtado-Lorenzo, A., Hosokawa, H., Zhuang, Z., Brown, D., Ausiello, D.A., Marshansky, V., 2011. Aldolase directly interacts with ARNO and modulates cell morphology and acidic vesicle distribution. Am. J. Physiol. - Cell Physiol. 300, 1442–1455. doi:10.1152/ajpcell.00076.2010.

Mosher, K.I., Schaffer, D.V., 2018. Influence of hippocampal niche signals on neural stem cell functions during aging. Cell Tissue Res 371, 115–124. doi:10.1007/s00441-017-2709-6.

O'Callaghan, J.P., Miller, D.B., 1991. The concentration of glial fibrillary acidic protein increases with age in the mouse and rat brain. Neurobiol. Aging 12, 171–174. doi:10.1016/0197-4580(91)90057-Q.

Olabarria, M., Noristani, H.N., Verkhratsky, A., Rodríguez, J.J., 2010. Concomitant astroglial atrophy and astrogliosis in a triple transgenic animal model of Alzheimer's disease. Glia NA-NA doi:10.1002/glia.20967.

Ottestad-Hansen, S., Hu, Q.X., Follin-Arbelet, V.V., Bentea, E., Sato, H., Massie, A., Zhou, Y., Danbolt, N.C., 2018. The cystine-glutamate exchanger (xCT, Slc7a11) is expressed in significant concentrations in a subpopulation of astrocytes in the mouse brain. Glia 66, 951–970. doi:10.1002/glia.23294.

Paxinos, G., Franklin, K.B.J., 2004. The Mouse Brain in Stereotaxic Coordinates, 2nd ed Elsevier Academic, London.

Piacentini, R., Li Puma, D.D., Mainardi, M., Lazzarino, G., Tavazzi, B., Arancio, O., Grassi, C., 2017. Reduced gliotransmitter release from astrocytes mediates tau-induced synaptic dysfunction in cultured hippocampal neurons. Glia 65, 1302–1316. doi:10.1002/GLIA.23163.

Popov, A., Brazhe, A., Denisov, P., Sutyagina, O., Li, L., Lazareva, N., Verkhratsky, A., Semyanov, A., 2021. Astrocyte dystrophy in ageing brain parallels impaired synaptic plasticity. Aging Cell 20, 1–14. doi:10.1111/acel.13334.

Reichenbach, A., Derouiche, A., Kirchhoff, F., 2010. Morphology and dynamics of perisynaptic glia. Brain Res. Rev. 63, 11–25. doi:10.1016/j.brainresrev.2010.02.003.

Reid, J.K., Kuipers, H.F., 2021. She doesn't even go here: the role of inflammatory astrocytes in CNS disorders. Front. Cell. Neurosci. 15, 1–12. doi:10.3389/fncel.2021.704884.

Rocchio, F., Tapella, L., Manfredi, M., Chisari, M., Ronco, F., Ruffinatti, F.A., Conte, E., Canonico, P.L., Sortino, M.A., Grilli, M., Marengo, E., Genazzani, A.A., Lim, D., 2019. Gene expression, proteome and calcium signaling alterations in immortalized hippocampal astrocytes from an Alzheimer's disease mouse model. Cell Death Dis 10, 24. doi:10.1038/s41419-018-1264-8.

Rodríguez-Arellano, J.J., Parpura, V., Zorec, R., Verkhratsky, A., 2016. Astrocytes in physiological aging and Alzheimer's disease. Neuroscience doi:10.1016/j.neuroscience.2015.01.007.

Rodríguez, J.J., Yeh, C.Y., Terzieva, S., Olabarria, M., Kulijewicz-Nawrot, M., Verkhratsky, A., 2014. Complex and region-specific changes in astroglial markers in the aging brain. Neurobiol. Aging 35, 15–23. doi:10.1016/j.neurobiolaging.2013.07.002.

Schiweck, J., Eickholt, B.J., Murk, K., 2018. Important shapeshifter: Mechanisms allowing astrocytes to respond to the changing nervous system during development, injury and disease. Front. Cell. Neurosci. 12, 261. doi:10.3389/fncel.2018.00261.

Scorcioni, R., Polavaram, S., Ascoli, G.A., 2008. L-Measure: a web-accessible tool for the analysis, comparison and search of digital reconstructions of neuronal morphologies. Nat. Protoc. 3, 866–876. doi:10.1038/nprot.2008.51.

SheikhBahaei, S., Morris, B., Collina, J., Anjum, S., Znati, S., Gamarra, J., Zhang, R., Gourine, A.V., Smith, J.C., 2018. Morphometric analysis of astrocytes in brainstem respiratory regions. J. Comp. Neurol. 526, 2032–2047. doi:10.1002/cne.24472.

Sheldon, A.L., Robinson, M.B., 2007. The role of glutamate transporters in neurodegenerative diseases and potential opportunities for intervention. Neurochem. Int. 51, 333–355. doi:10.1016/J.NEUINT.2007.03.012.

Sonne, J., Reddy, V., Beato, M.R., 2020. Neuroanatomy, Substantia Nigra. StatPearls, Treasure Island (FL).

Soreq, L., Rose, J., Soreq, E., Hardy, J., Trabzuni, D., Cookson, M.R., Smith, C., Ryten, M., Patani, R., Ule, J., 2017. Major shifts in glial regional identity are a transcriptional hallmark of human brain aging. Cell Rep 18, 557–570. doi:10.1016/j.celrep.2016.12.011.

Spampinato, S.F., Bortolotto, V., Canonico, P.L., Sortino, M.A., Grilli, M., 2019. Astrocyte-derived paracrine signals: relevance for neurogenic niche regulation and blood-brain barrier integrity. Front. Pharmacol. 10, 1346. doi:10.3389/fphar.2019.01346.

Tanner, C.M., Goldman, S.M., 1996. Epidemiology of Parkinson's disease. Neurol. Clin. 14, 317–335. doi:10.1016/S0733-8619(05)70259-0.

Venkateshappa, C., Harish, G., Mythri, R.B., Mahadevan, A., Srinivas Bharath, M.M., Shankar, S.K., 2012. Increased oxidative damage and decreased antioxidant function in aging human substantia Nigra compared to striatum: implications for Parkinson's disease. Neurochem. Res. 37, 358–369. doi:10.1007/s11064-011-0619-7.

Verkerke, M., Hol, E.M., Middeldorp, J., 2021. Physiological and pathological ageing of astrocytes in the human brain. Neurochem. Res. 46, 2662–2675. doi:10.1007/s11064-021-03256-7.

Verkhratsky, A., Augusto-Oliveira, M., Pivoriūnas, A., Popov, A., Brazhe, A., Semyanov, A., 2020. Astroglial asthenia and loss of function, rather than reactivity, contribute to the ageing of the brain. Pflugers Arch. Eur. J. Physiol. 473, 753–774. doi:10.1007/s00424-020-02465-3.

Verkhratsky, A., Nedergaard, M., 2018. Physiology of astroglia. Physiol. Rev. 98, 239–389. doi:10.1152/physrev.00042.2016.

Verkhratsky, A., Parpura, V., Li, B., Scuderi, C., 2021. Astrocytes: the housekeepers and guardians of the CNS. Adv. Neurobiol. 26, 21–53. doi:10.1007/978-3-030-77375-5_2.

Verkhratsky, A., Zorec, R., Rodríguez, J.J., Parpura, V., 2016. Astroglia dynamics in ageing and Alzheimer's disease. Curr. Opin. Pharmacol. 26, 74–79. doi:10.1016/j.coph.2015.09.011.

Volker, K.W., Knull, H.R., 1997. A glycolytic enzyme binding domain on tubulin. Arch. Biochem. Biophys. 338, 237–243. doi:10.1006/ABBI.1996.9819.

Wickham, H., 2016. ggplot2. Use R! Springer International Publishing, Cham doi:10.1007/978-3-319-24277-4.

Wickham, H., Averick, M., Bryan, J., Chang, W., McGowan, L.D., François, R., Grolemund, G., Hayes, A., Henry, L., Hester, J., Kuhn, M., Pedersen, T.L., Miller, E., Bache, S.M., Müller, K., Ooms, J., Robinson, D., Seidel, D.P., Spinu, V., Takahashi, K., Vaughan, D., Wilke, C., Woo, K., Yutani, H., D', L., Mcgowan, A., François, R., Grolemund, G., Hayes, A., Henry, L., Hester, J., Kuhn, M., Lin Pedersen, T., Miller, E., Bache, S.M., Müller, K., Ooms, J., Robinson, D., Seidel, D.P., Spinu, V., Takahashi, K., Vaughan, D., Wilke, C., Woo, K., Yutani, H., 2019. Welcome to the tidyverse. J. Open Source Softw 4, 1686. doi:10.21105/JOSS.01686.

Yeh, C.Y., Vadhwana, B., Verkhratsky, A., Rodríguez, J.J., 2011. Early astrocytic atrophy in the entorhinal cortex of a triple transgenic animal model of Alzheimer's disease. ASN Neuro 3, 271–279. doi:10.1042/AN20110025.